Plasmid stability in fluctuating environments: population genetics of multi-copy plasmids

V Miró Pina[1, 2,†], JCR Hernandez-Beltran[3,4,†], A Siri-Jégousse[5], S Palau[5], R Peña-Miller[3], and A González Casanova[6,*]

[1] Centre for Genomic Regulation (CRG), The Barcelona Institute of Science and Technology, Barcelona, Spain
[2] Universitat Pompeu Fabra (UPF), Barcelona, Spain
[3] Laboratorio de Biología de Sistemas, Centro de Ciencias Genómicas, Universidad Nacional Autónoma de México, 62210, Cuernavaca, México
[4] Department of Microbial Population Biology, Max Planck Institute for Evolutionary Biology, 24306 Plön, Germany
[5] Departamento de Probabilidad y Estadística, Instituto de Investigación en Matemáticas Aplicadas y en Sistemas, Universidad Nacional Autónoma de México, México
[6] Instituto de Matemáticas, Universidad Nacional Autónoma de México, México
[†]These authors contributed equally
[*]Corresponding author: adriangcs@matem.unam.mx

ABSTRACT

Plasmids are extra-chromosomal genetic elements that encode a wide variety of phenotypes and can be maintained in bacterial populations through vertical and horizontal transmission, thus increasing bacterial adaptation to hostile environmental conditions like those imposed by antimicrobial substances. To circumvent the segregational instability resulting from randomly distributing plasmids between daughter cells upon division, non-transmissible plasmids tend to be carried in multiple copies per cell, with the added benefit of exhibiting increased gene dosage. But carrying multiple copies also results in a high metabolic burden to the bacterial host, therefore reducing the overall fitness of the population. This trade-off poses an existential question for plasmids: What is the optimal plasmid copy number? In this manuscript, we address this question using a combination of population genetics modeling with microbiology experiments consisting of *Escherichia coli* K12 bearing a multi-copy plasmid encoding for $bla_{\text{TEM-1}}$, a gene conferring resistance to β-lactam antibiotics. We postulate and analyze a Wright-Fisher model to evaluate the interaction between selective pressure, the number of plasmid copies carried by each cell, and the energetic cost associated with plasmid bearing. By numerically determining the optimal plasmid copy number for constant and fluctuating selection regimes, we show that the stability of multi-copy plasmids is maximized at intermediate plasmid copy numbers. We conclude by arguing that plasmid copy number is a highly optimized evolutionary trait that depends on the rate of environmental fluctuation and balances the benefit between increased stability in the absence of selection with the burden associated with carrying multiple copies of the plasmid.

Keywords: Multi-copy plasmids, Wright-Fisher model, Experimental microbiology, Optimal plasmid copy number

1 Introduction

Prokaryotes transfer DNA at high rates within microbial communities through mobile genetic elements such as bacteriophages,[1] transposons[2] or extra-chromosomal DNA molecules known as plasmids.[3] Crucially, plasmids have core genes that allow them to replicate independently of the chromosome but also encode for accessory genes that provide their bacterial hosts with new functions and increased fitness in novel or stressful environmental conditions.[4] Plasmids have been widely studied due to their biotechnological potential[5] and their relevance in agricultural processes,[6] but also because of their importance in clinical practice since they have been identified as significant factors contributing to the current global health crisis generated by drug resistance of clinically-relevant pathogens.[7]

It is generally assumed that, in the absence of selection for plasmid-encoded genes, most plasmids impose a burden for their bacterial hosts.[8,9] As a result, plasmid-bearing populations usually have a competitive disadvantage against plasmid-free cells, thus threatening plasmids to be cleared from the population through purifying selection.[10] To avoid extinction, some plasmids overcome segregational instability by transmitting horizontally to lineages with increased fitness, with previous theoretical results establishing sufficient conditions for plasmid maintenance, namely that the rate of horizontal transmission has to be larger than the combined effect of segregational loss and fitness cost.[11,12] Also, some plasmids encode molecular mechanisms that increase their stability, for instance, toxin-antitoxin systems that kill plasmid-free cells,[13] or active partitioning mechanisms that ensure the symmetric segregation of plasmids upon division.[14]

To circumvent segregational loss, non-conjugative plasmids lacking active partitioning and post-segregational killing mechanisms tend to be present in many copies per cell, therefore, decreasing the probability of producing a plasmid-free cell when randomly segregating plasmids during cell division. But this reduced rate of segregational loss is not sufficient to explain the stable persistence of costly plasmids in the population, suggesting that a necessary condition for plasmids to persist in the population is to carry beneficial genes for their hosts that are positively selected for in the current environment. However, regimes that positively select for plasmid-encoded genes can be sporadic and highly specific, so plasmid persistence is not guaranteed in the long term. Moreover, even if a plasmid carries useful genes for the host, these can be captured by the chromosome, thus making plasmids redundant and rendering them susceptible to be cleared from the population.[15]

While the benefits of carrying plasmids may be clear under certain circumstances, it is also patent that their maintenance can be associated with a considerable energetic cost. For instance, increasing plasmid copy number results in an increase in gene dosage and a reduced probability of plasmid loss, but can also be associated with a larger fitness cost in the absence of selection for plasmid-encoded genes. This trade-off between segregational stability and fitness cost has been shown to drive ecological and evolutionary dynamics in plasmid-bearing populations,[16] resulting from multi-level selection acting

on extrachromosomal genetic elements.[17,18] As a result, a series of theoretical and experimental studies have proposed that non-transmissible plasmids must provide additional benefits for plasmid-bearing populations, with important consequences in the ecological and evolutionary dynamics of bacterial populations.[19]

Of note, as multi-copy plasmids are present in numerous copies per cell, the mutational target increases considerably and, once a beneficial mutation appears, its expression is amplified during plasmid replication. This results in an accelerated rate of adaptation to adverse environmental conditions[7] and enables evolutionary rescue.[20] Also, multi-copy plasmids increase the genetic diversity of the population, thus enhancing survival in fluctuating environments and allowing bacterial populations to circumvent evolutionary trade-offs.[21] Furthermore, random segregation and replication of plasmids produce a complex interaction between plasmid copy number, genetic dominance, and segregational drift, with important consequences in the fixation probability of beneficial mutations[22] and the repertoire of genes that can be carried in mobile genetic elements.[23]

In this paper, we use a classic Wright-Fisher modeling approach to evaluate the interaction between the number of plasmid copies contained in each cell and the energetic cost associated with carrying each plasmid copy. We will assume that this is a non-transmissible, multi-copy plasmid (it can only be transmitted vertically) and that it lacks active partitioning or post-segregational killing mechanisms (plasmids segregate randomly upon division). We will also consider that plasmids encode for a gene that increases the probability of survival to an otherwise lethal concentration of an antimicrobial substance. We use computer simulations to evaluate plasmid stability as a function of the duration and strength of selection in favor of this plasmid-encoded resistance gene. This will allow us to estimate the plasmid copy number that maximizes plasmid stability under different environmental regimes: drug-free environments, constant exposure to a lethal drug concentration, and intermittent periods of selection.

To validate our theoretical results, we will use an experimental model system consisting on *Escherichia coli* carrying a multi-copy plasmid pBGT ($\sim$19 copies per cell) encoding $bla_{\text{TEM-1}}$, a drug-resistance gene that produces a β-lactamase that degrades ampicillin and other β-lactam antibiotics.[7,24] pBGT also encodes for a GFP fluorescent marker, and therefore we can obtain time-resolved estimates on the fraction of plasmid-bearing cells present in the population using a spectrophotometer. Specifically, here we will perform competition experiments under a range of drug concentrations (a β-lactam antibiotic, ampicillin) with different initial fractions of plasmid-bearing and plasmid-free cells, thus providing estimates on key parameters of our population genetics model.

Both our model and the experimental results confirm the existence of two opposing evolutionary forces acting on the number of copies carried by each cell: selection against high-copy plasmids consequence of the fitness cost associated with bearing multiple copies of a costly plasmid, and purifying selection resulting from the increased probability of plasmid loss observed in low-copy plasmids. We

conclude by arguing that, as the existence of plasmids in natural environments requires intermittent periods of positive selection, the presence of plasmids contains information on the environment on which a population has evolved. Indeed, the plasmid copy number associates the frequency of selection with the energetic costs of plasmid maintenance. That is, there is a minimum frequency of drug exposure that allows multiple copies to persist in the population, and, for each environmental regime, there is an optimal number of plasmid copies.

The Model

A Wright-Fisher model for multi-copy plasmid dynamics

We consider a discrete-time Wright-Fisher process to model the evolution of a population of fixed size N, with two types of individuals: plasmid-bearing (PB) and plasmid-free (PF). Let us denote by n the plasmid copy number (PCN) and argue that this is an important parameter: in the one hand, the selective disadvantage of PB individuals due to the cost of carrying plasmids is assumed to be proportional to n; on the other hand, the PCN determines the heritability of the plasmid.

At the moment of cell division, each plasmid is randomly segregated into one of the two new cells, and, once in the new host, the plasmids replicate until reaching n copies. If, however, one of the two new cells has all the n copies, the other one will not carry any plasmid copies and therefore becomes PF. This means that the daughter of a PB cell becomes PF with probability $\mu_n = 2^{-n}$ (segregational loss rate). As a consequence, plasmids are readily cleared from the population when the number of copies is low, and the rate of plasmid loss decreases exponentially with n. Segregational loss can be seen, in a Wright-Fisher model as "mutations" from PB to PF at rate μ_n.

We also consider that the fitness cost associated with plasmid maintenance is a constant multiplied by n. In the Wright-Fisher model, this would correspond to PB individuals having some selective disadvantage κ_n. Formally, if $X_i^{(N)}$ is the proportion of PB individuals at generation i, each individual at generation $i+1$ chooses a PB parent with probability

$$\frac{(1-\kappa_n)X_i^{(N)}}{(1-\kappa_n)X_i^{(N)} + 1 - X_i^{(N)}}.$$

Since the cost of plasmid is very large compared to $1/N$ (i.e. $\kappa_n = \kappa n$), we are in the case of strong selection (see[25] and Appendix A). The frequency process of PB individuals converges, when $N \to \infty$, to a discrete time deterministic sequence defined in a recursive way as

$$X_{i+1} = f(X_i) := \frac{(1-\kappa_n)X_i}{(1-\kappa_n)X_i + 1 - X_i}(1-\mu_n), \qquad i \geq 1. \tag{1}$$

1.1 Modeling the introduction of antibiotics

Additionally, we aim at modelling selection for plasmid-encoded genes. For plasmids that encode antibiotic resistance genes, this is achieved by treating the population with antibiotic pulses. Individuals with no plasmids are more exposed to this treatment and at each pulse we observe an increment of the relative frequency of the plasmid-bearing population. To model this phenomenon, we assume that, in the presence of antibiotic, PF individuals have some selective disadvantage $\alpha \in [0,1]$.

If the antibiotic pulse occurs at generation i, the fraction of PB individuals before reproduction becomes

$$g(X_i) := \frac{X_i}{X_i + (1-\alpha)(1-X_i)}.$$

Then, after reproduction, the frequency of PB individuals at the next generation is $X_{i+1} = f(g(X_i))$. Finally, considering that the pulses occur at generations $T, 2T, \ldots$, the frequency process becomes

$$X_{i+1} = \begin{cases} f(g(X_i)) = \frac{(1-\kappa_n)X_i}{1-\alpha+(\alpha-\kappa_n)X_i}(1-\mu_n) & \text{if } i = jT, \ \ j = 1,2\ldots \\ f(X_i) = \frac{(1-\kappa_n)X_i}{(1-\kappa_n)X_i+1-X_i}(1-\mu_n) & \text{otherwise.} \end{cases} \tag{2}$$

Serial dilution protocol

The assumption of constant population size seems far from reasonable, specially in a serial dilution protocol. There had been several attempts to adapt the classical theory of Wright Fisher models to this experimental setting (see for example[26]). A mathematical rigorous way to do this was developed in.[27] In[28] an heuristic and applicable to data framework was introduced. Recently, in,[29] the two methodologies had been paired in order to have a rigorous and applicable way to use classic population genetics to study experiments. In this work, days take the role of generations, and as the number of individuals after each sampling is more or less constant, the assumption of constant population size becomes reasonable.

Each day starts with a population of N cells that grow exponentially until saturation is reached (i.e. until there are γN cells.). The reproduction rate (or *Malthusian fitness*) of PB (resp. PF) individuals is r (resp. $r+\rho$), with $\rho > 0$ (since PB individuals have some disadvantage due to the cost of plasmid maintenance). The duration of the growth phase is $\sigma \simeq \log(\gamma)/r$.

This fluctuations in the population size modify the effective "mutation" and "selection" parameters κ_n and μ_n, which need to be suitable calculated taking by analytic tools that into account the intra-day dynamics of the population. In Appendix A we detail how this correspondence is made.

In our case, the population behaves as in (2), where each generation is one day and

$$\kappa_n = \frac{\rho(1-e^{-(r2^{-n}+\rho)\sigma})}{r2^{-n}+\rho} \qquad \text{and} \qquad \mu_n = 1 - \frac{r2^{-n}+\rho}{r2^{-n}e^{(r2^{-n}+\rho)\sigma}+\rho}. \tag{3}$$

The importance of this formulas is that they breach measurable quantities with theoretical parameters, leading to a method to estimate the parameters of the model from experiments, which is spirit of the experiment that we designed and performed.

2 Results

Segregational instability in the absence of selection

First, we focused on segregational instability in the absence of selection for plasmid-encoded genes (i.e. without antibiotics). By numerically solving equation (1), we studied the stability of plasmids in terms of the mean plasmid copy number (PCN) and the fitness cost associated with carrying each plasmid copy (κ). As expected, in the absence of selection, plasmids are always cleared from the population with a decay rate that depends on PCN. We define the time-to-extinction as the time when the fraction of plasmid-bearing (PB) cells goes below an arbitrary threshold.

For cost-free plasmids (i.e. when $\kappa = 0$), the time-to-extinction appears to be correlated to PCN as illustrated in Figure 1A. In contrast, if we consider costly plasmids ($\kappa > 0$) and that the total fitness cost is proportional to the PCN (i.e. if $PCN = n$, the total cost is $\kappa_n = \kappa n$), then extinction occurs in a much faster timescale (Figure 1B – notice the difference of timescales with Figure 1A). As shown in Figure 1B, small PCN values are associated with a high probability of segregational loss, and therefore the time-to-extinction increases with PCN. However, large values of PCN are associated with higher levels of instability due to the detrimental effect on host fitness resulting from carrying multiple copies of a costly plasmid.

This observation indicates the existence of a non-linear relationship between stability of plasmids and the mean PCN of the population. To further explore this relationship, we estimated computationally the time-to-extinction in a long-term setting (simulations running up to 500 days) for different values of PCN and fitness cost. Figure 1C shows an accelerated rate of plasmid loss in costly plasmids. Crucially, there appears to be a critical PCN that maximizes the time-to-extinction, that depends on the per-cell plasmid cost. The time-to-extinction gives a notion of the stability of plasmids, but this measure may not apply if we introduce antibiotics, and therefore avoid plasmid extinction. For this reason we quantified plasmid stability by measuring area under the curve (AUC) of simulation trajectories similar to those in Figure 1B. Figure 1D illustrates the existence of a region in the cost-PCN plane, at intermediary PCN values, where plasmid stability is maximized.

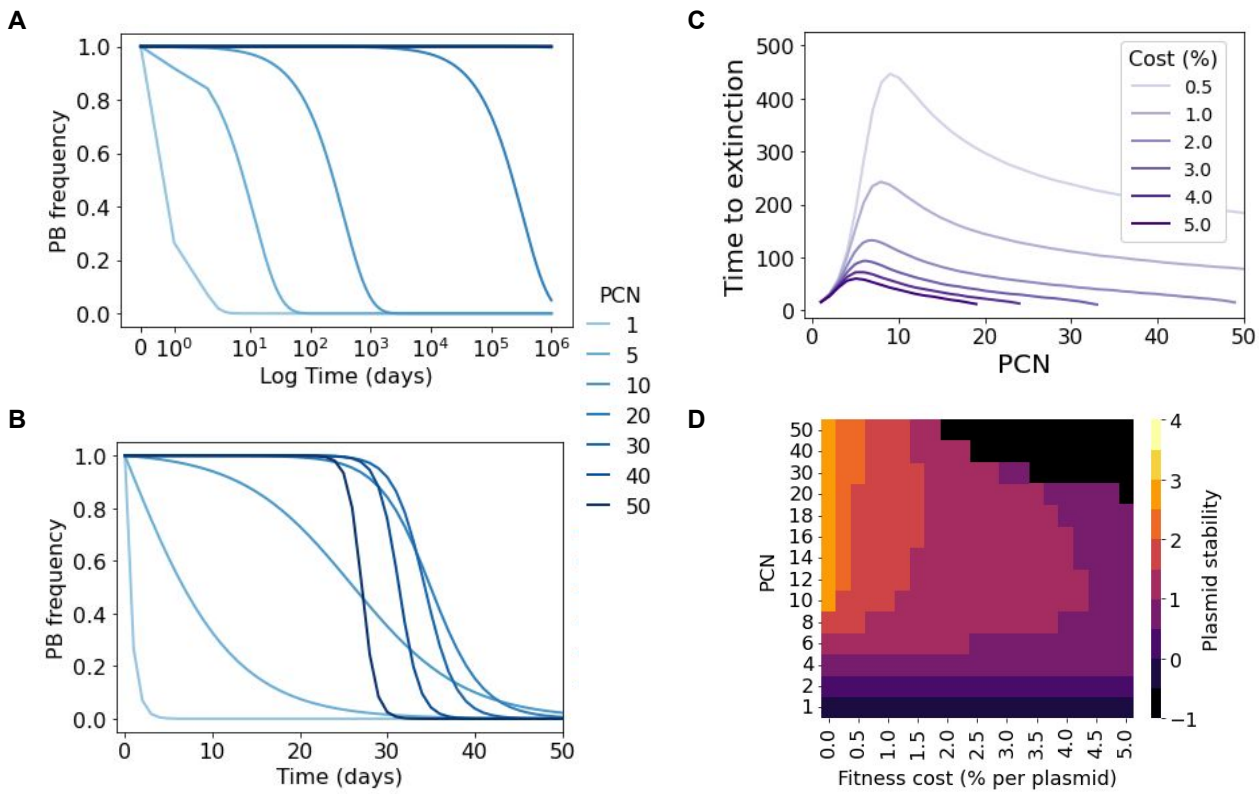

Figure 1. Numerical results for the model without selection for plasmid-encoded genes. A) Plasmid frequency as a function of time for a cost-free plasmid ($\kappa = 0$). Note how, as the PCN increases, the stability of plasmids also increases, although eventually all plasmids will be cleared from the system. **B)** Dynamics of plasmid loss for strains bearing a costly plasmid ($\kappa = 0.0143$). In this case, low-copy plasmids (light blue lines) are highly unstable, but so are high-copy plasmids (dark blue lines). **C)** Time elapsed before plasmid extinction for a range of PCNs. A very costly plasmid ($\kappa = 5\%$) is represented in dark purple, while the light purple line denotes a less costly plasmid ($\kappa = 0.5\%$). **D)** Plasmid stability for a range of fitness costs and plasmid copy numbers (discrete colormap indicates level of stability, yellow denotes higher stability, while dark purple denotes rapid extinction). Stability is measured as the area under the curve (AUC) of trajectories similar to those in **B**, expressed in $\log_{10}$ scale. Notice that, for intermediate fitness costs, the PCN that maximizes plasmid stability can be found at intermediate values.

Evaluating the role of selection in the stability of plasmids

To study the interaction between plasmid stability and the strength of selection in favor of PB cells, our model considers that the plasmid carries a gene that confers a selective advantage to the host in certain environments (e.g. resistance to heavy metals or antibiotics). For the purpose of this study, we will consider a bactericidal antibiotic that kills PF cells with a probability that depends on the antibiotic dose, resulting in a competitive advantage of the PB cells with respect to PF ones in this environment. We denote the intensity of this selective pressure by α.

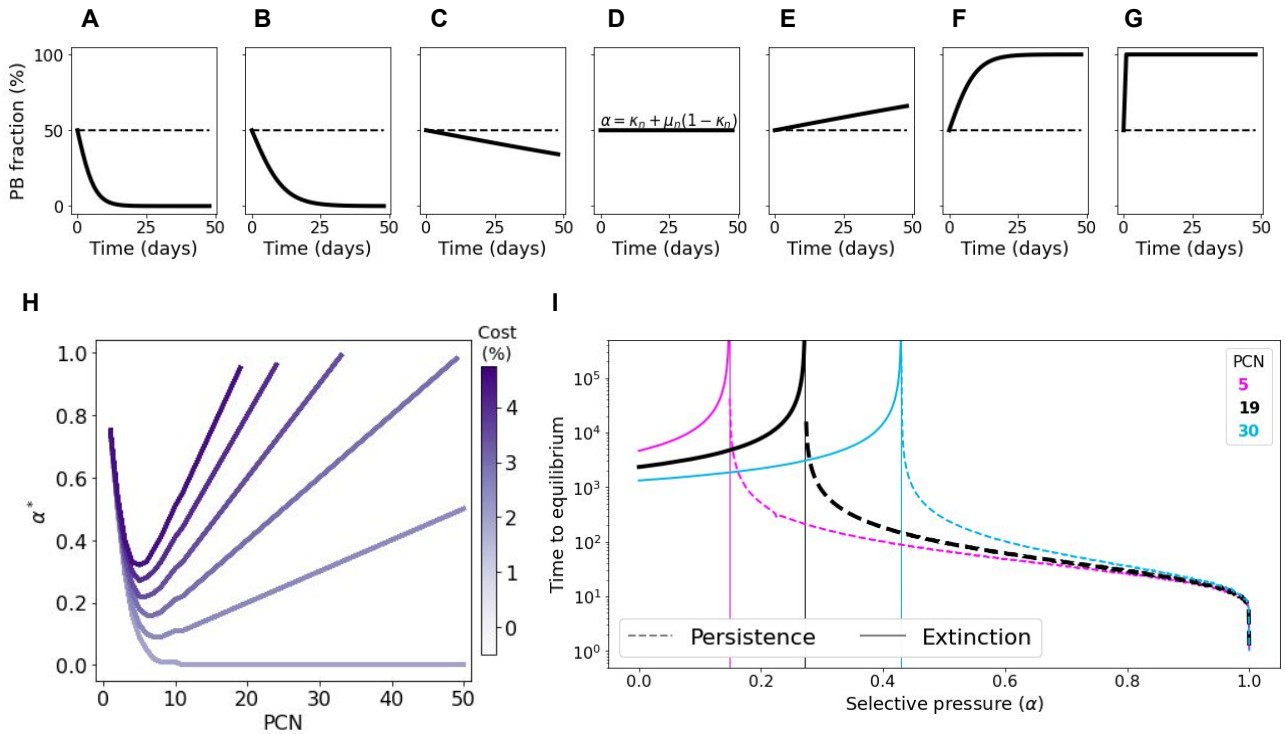

Figure 2. Numerical results illustrating the effect of a constant selective pressure in the stability of non-transmissible multi-copy plasmids. A-G) Each box illustrates the temporal dynamics of the plasmid-bearing subpopulation in a pairwise competition experiment inoculated with equal initial fractions of PF and PB. From left to right, $\alpha = 0, 0.2, 0.26, 0.28, 0.6$ and 1. The dotted line denotes $\alpha^* = \kappa_n + \mu_n(1-\kappa_n)$ for $n = 19$ and $\kappa_n = 0.27$. Note that for values of $\alpha < \alpha^*$, plasmids are unstable and eventually cleared from the population, while for $\alpha > \alpha^*$ the plasmid-bearing subpopulation increases in frequency until reaching fixation. For $\alpha = \alpha^*$, the selective pressure in favor of the plasmid compensates its fitness cost and therefore the plasmid fraction remains constant throughout the experiment. **H)** Minimum selective pressure required to avoid plasmid loss for a range of plasmid copy numbers. Different curves represent plasmids with different fitness costs (light purple denotes cost-free plasmids and dark purple a very costly plasmid). Note that, for costly plasmids, there exists a non-monotone relationship between α^* and PCN. **I)** Time elapsed before plasmid fraction in the population is stabilized, for a range of copy numbers (5 in magenta, 19 in black, and 30 in cyan). Dotted lines represent plasmid fixation, while dashed lines denote stable co-existence between plasmid-free and plasmid-bearing subpopulations, and solid lines plasmid extinction. The vertical line indicates α^*, the minimum selective pressure that stably maintains plasmids in the population. Black letters indicate the parameter values used in the examples shown in A-G.

Figures 2A-G illustrate plasmid dynamics over time for different values of α, obtained by numerically solving equation (2) with a fixed PCN ($n = 19$) and drug always present in the environment ($T = 1$). In our model, the critical dose that stabilizes plasmids in the population corresponds to $\alpha^* = \kappa_n + \mu_n(1 - \kappa_n)$ (see Appendix A). The existence of a minimum antibiotic dose that maintains plasmids in the population is a feature used routinely by bioengineers to stabilize plasmid vectors through selective media.[30] As illustrated in Figure 2H, both low-copy and high-copy plasmids are inherently unstable and therefore the selective pressure necessary to stabilize them is relatively high, particularly for costly plasmids. Interestingly, at intermediate PCN values, the selective conditions necessary to stabilize plasmids are considerably less stringent than for low- and high-copy plasmids. This is the result of the non-linear relationship between α^* and n; since μ_n decreases exponentially with n, while κ_n increases only linearly with n.

Figure 2I shows the time elapsed before converging to the steady-state (either extinction or persistence) for different values of α and PCN. As α increases, the cost of plasmid-bearing is compensated by the benefit of carrying the plasmid and therefore plasmids are maintained in the population for longer. Note that at large values of α, plasmid-free cells are killed immediately independently of the mean PCN of the population, resulting very fast in a population composed almost exclusively of plasmid-bearing cells. The equilibrium fraction $x^* = 1 - \mu_n \frac{1-\kappa_n}{\alpha-\kappa_n}$ is achieved independently of the initial fraction of PB cells (see Appendix A), which is consistent with previous results.[31]

Experimental model system: a non-transmissible, multi-copy plasmid encoding for a resistance gene

Our model allows to make predictions on how the long-term evolution of plasmid-bearing populations depends on plasmid cost and fitness advantage conferred by the plasmid in certain environments. We aim at quantifying these parameters experimentally. However, a long-term evolutionary experiment would produce changes such as compensatory mutations[32,33] or plasmid genes integrating into the chromosome.[15] To overcome this limitation, we designed a simple one-day competition experiment whereby we artificially mixed PB and PF subpopulations at different initial fractions, and exposed them to a gradient of antibiotics.

In particular, here we used *Escherichia coli* MG1655 carrying pBGT, a non-transmissible multi-copy plasmid used previously to study plasmid dynamics and drug resistance evolution.[21,34,35] Briefly, pBGT is a ColE1-like plasmid with $\sim$19 plasmid copies per cell, lacking the necessary machinery to perform conjugation or to ensure symmetric segregation of plasmids upon division. This plasmid carries a GFP reporter under an arabinose inducible promoter and the $bla_{\text{TEM-1}}$ gene that encodes for a β-lactamase that efficiently degrades β-lactam antibiotics, particularly ampicillin (AMP). The minimum inhibitory concentration (MIC) of PB cells to AMP is $8,192$ mg/l, while the PF strain has a MIC of 4 mg/l (see Appendix B).

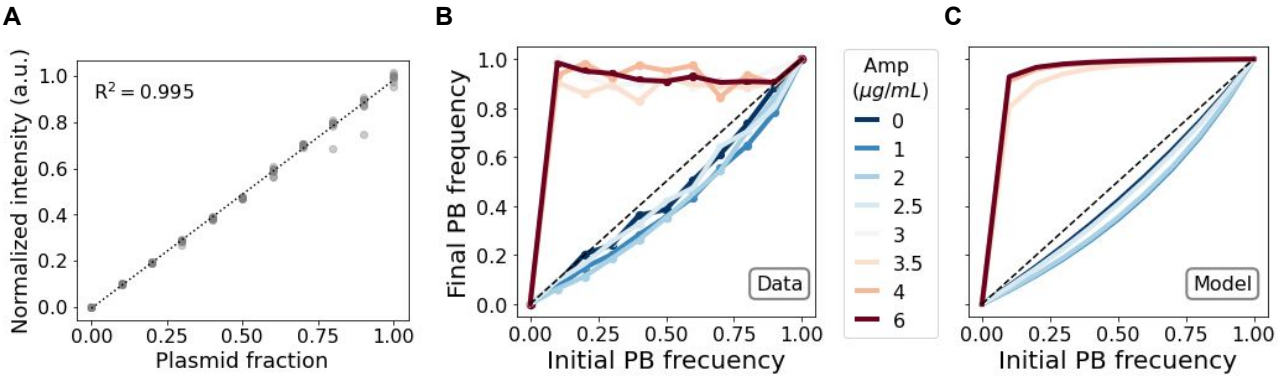

Figure 3. Model parametrization. A) Plasmid fraction estimation. Different fractions of artificially mixed populations of PB and PF strains vs the normalized fluorescence intensity of such populations. Each dot present a replica and the dotted line is a linear regression with R^2=0.995. **B)** Competition experiments of the same populations submitted to a range of ampicillin concentrations (0, 1, 2, 2.5, 3, 3.5, 4, and 6 $\mu g/ml$) indicated by different colors. **C)** Simulations using equation (2). Parameters κ_n and α were estimated using a curve fitting algorithm. Plasmid cost, κ_n, was calculated from the experimental curve without antibiotics. Fixing κ_n we fitted the values of α for different antibiotic concentrations (see Table 2). Colors indicate antibiotic concentrations. Blues represent concentrations where effect of plasmid cost is stronger than the effect of selection, yielding curves below the identity line. Reds represent concentrations where selection kills PF strain.

To quantify the fitness cost associated with carrying multiple copies of pBGT, we performed growth experiments in 96-well plates where each strain was grown in lysogeny broth (LB) rich media. We obtained approximate values for the maximal growth rates of the PB and PF strains corresponding to r and ρ in the intraday model (see[36] and Appendix B). So, if a reduction in bacterial fitness is expressed in terms of a decrease in its maximum growth rate, then the metabolic burden associated with carrying the pBGT plasmid is 0.108 ± 0.067.

Moreover, we measured the plasmid cost and the decrease in competitive fitness associated to antibiotics in our interday model. To do so, we used the normalized fluorescent intensity as a proxy for the proportion of PB cells (Figure 3A shows a linear relationship between both quantities) and then performed growth experiments starting with different initial fractions of PB cells, with end points shown in Figure 3B. In the absence of antibiotic, since the PCN is fixed, the PB fraction at the end of the day only depends on the plasmid cost. By fitting equation (1), we obtained $\kappa_n = 0.272$. Moreover, by fixing this parameter and incorporating antibiotics, we estimate the selective pressure α for different antibiotic concentrations by fitting equation (2) (Figures 3B and 3C). Table 1 summarizes parameter values estimated for each strain in our model and Table 2 shows the correspondence between antibiotic concentrations and α.

In our experiments, we also observed that low antibiotic concentrations (small values of α) yield a decrease in the PB frequency, while higher concentrations yield an increase in the PB frequency. This is consistent with the existence of a critical antibiotic dose to promote plasmid persistence in constant environments observed in Figure 2.

Plasmid stability in periodic environments

The aim of this section is to understand the evolutionary dynamics of the plasmid-bearing population in fluctuating environments, i.e. when periodic antibiotic pulses are administered. We started by exploring how much time a PB population can survive without antibiotics before being rescued by a strong antibiotic pulse (Figure 4A). Consistently with the results from the first section, lower plasmid costs showed increased rescue times. This introduced the notion that a certain rate of antibiotic pulses would be required for plasmid maintenance. In Figure 4B, we quantified this minimal period as a function of PCN and α. Note that higher values of α correspond to longer periods, which follows from the fact that a higher selective pressure increases the PB frequency. Figure 4D illustrate this minimal period for $PCN = 19$.

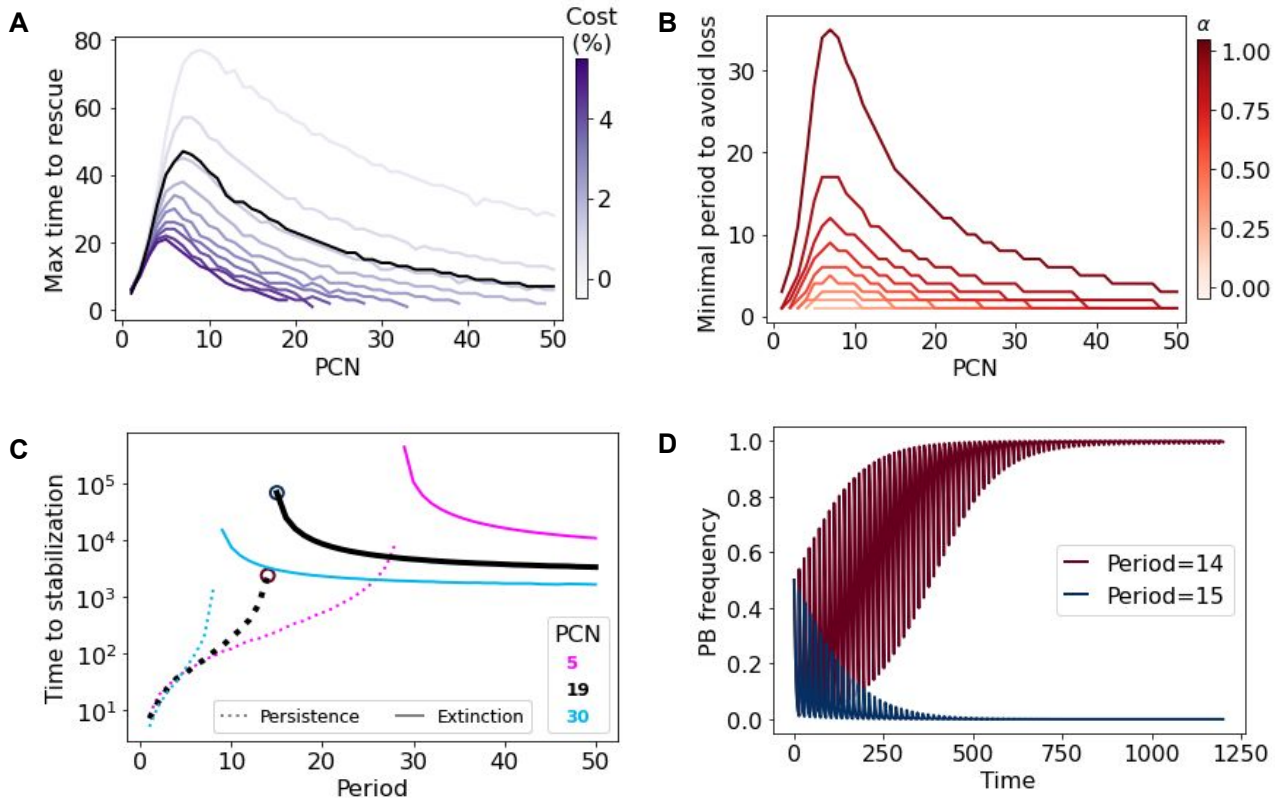

Figure 4. Numerical results of the model in periodic environments. A) Maximum time a plasmid population can grow without antibiotics to avoid plasmid loss when applying a strong antibiotic pulse. Curves represent how this time is affected by PCN. Blue intensity represents plasmid cost, and black line indicates results using the pBGT parameters. **B)** Minimal period required to avoid plasmid extinction. Simulations were performed using the pBGT measured cost ($\kappa = 0.014$). Red intensity represents different values of α. Note that higher values of α increase the minimal period. **C)** Time required for trajectories to stabilize for copy numbers 5, 19, and 30 using $\alpha = 0.99$ and the measured cost per plasmid. Note that there is a critical period that defines fixation or coexistence marked by red and blue circles on the PCN=19 (black) curve. **D)** Trajectories for the critical periods of PCN=19 starting from 0.5 PB-PF frequency. Note that one day period difference leads to opposite outcomes.

In periodic environments, the PB population will either go extinct or reach a steady state in which the plasmid fraction oscillates around an equilibrium frequency (persistence). In Figure 4C, times to stabilization were estimated for the strong selection regime ($\alpha = 0.99$) using the same PCNs as in Figure 2. Notice that the time-to-extinction is shorter than the time to reach the periodic attractor.

For both the maximal time for rescue and the minimal period to avoid loss, we observe a range of plasmid copy numbers where plasmid stability is maximized. This is consistent with what we observed without antibiotics (Figure 1C) and with constant environments (Figure 2). In the next section, we will explore the concept of optimal PCN.

Optimal PCN depends on the rate of environmental fluctuation

In this section, we aim at exploring concept of optimal PCN and how it depends on the environment. To do so, we define the optimal PCN (hereafter denoted PCN*), as the PCN that maximizes the area under the curve (AUC) of the PB frequency over time. This notion of stability was already introduced in Figure 1D and has the advantage that it can be used when the PB fraction goes to 0, to a fixed equilibrium or when it oscillates.

First, we used an antibiotic-free regime to calculate PCN* for a range of plasmids fitness costs (black solid line of Figure 5A). We found that PCN* is inversely correlated with the plasmid fitness cost in an exponential manner. We compared the optimal PCN to values of PCN found in nature. Although it is not common to find studies that measure both PCN and fitness cost, we found a few of them (summarized in Table 4). These values are marked as black dots in Figure 5A, while the red dots represent the pBGT plasmid used in our experiments. Notably, the values of PCN found in the literature were below our predicted PCN* in an antibiotic-free regime. However they are within the blue-shaded area that represents the PCN* for a range of antibiotic concentrations applied daily (observe the non-linear relationship between α, PCN* and cost, in line with our previous findings).

These observations would be consistent with a constant use of antibiotics at low doses that reduces the optimal PCN. However, similar PCN* values can be achieved by administering higher doses of antibiotics periodically, as illustrated in Figure 5B for the case of pBGT. Notice again the non-linear relationship between PCN* and the frequency of antibiotic exposure. At very low frequencies, the PB population goes extinct before the first antibiotic pulse and intermediate PCNs maximize the AUC as in Figure 1D. At high antibiotic frequencies, the PB population persists and oscillates around some value that increases with PCN. This is consistent with a previous experimental study that evaluated the stability of costly plasmid in terms of the frequency of positive selection.[37]

Periodic environments gave us insights on how selection acts on PCN, with results that can be used to design rational treatments that suppress plasmid-mediated antibiotic resistance.[38] But natural environments are not periodic but highly variable, with alternating intervals of positive and

negative selection. To explore this, we created stochastic environments that randomly switch from antibiotic-free to a lethal dose of antibiotic for a period of 1000 days. In our model, each random environment can be represented by a sequence of 1s and 0s, corresponding to days with and without antibiotic, respectively. Therefore stochastic environments can be characterized by their Shannon's entropy (environmental entropy, H) and the fraction of antibiotic days (namely antibiotic rate, AR) (see Appendix B). Environments were classified into "High" and "Low" depending on whether the AR was greater or lower than 0.5. Mind that each value of H corresponds to two AR values R and $1-R$ (see Supplementary Figure 1).

The panels on Figures 5D-E show the PCN* found by applying the stochastic environments ordered by entropy or by AR, for different values of α. For low values of α, only high antibiotic rates lead to plasmid persistence. Notice the non-linear relationship between PCN* and AR, similar to the one observed for the period in the deterministic setting: PCN* decreases with AR at low values (corresponding to extinction) but increases with AR at high values, corresponding to persistence. For higher values of α, we observe that high AR always leads to persistence, while low AR can lead to extinction if entropy is low. In fact, these low values of the entropy correspond to long periods without antibiotic, in which the PB population goes to extinction. Another interesting remark is that the distribution of obtained PCN*s is clearly multi-modal: at fixed entropy, plasmid persistence is achieved by high values of AR that correspond to high PCN* , or by low values of AR that correspond to a small value of PCN*. Similarly, a fixed value of α corresponds to two values of PCN* depending on the antibiotic rate (Figure 5C).

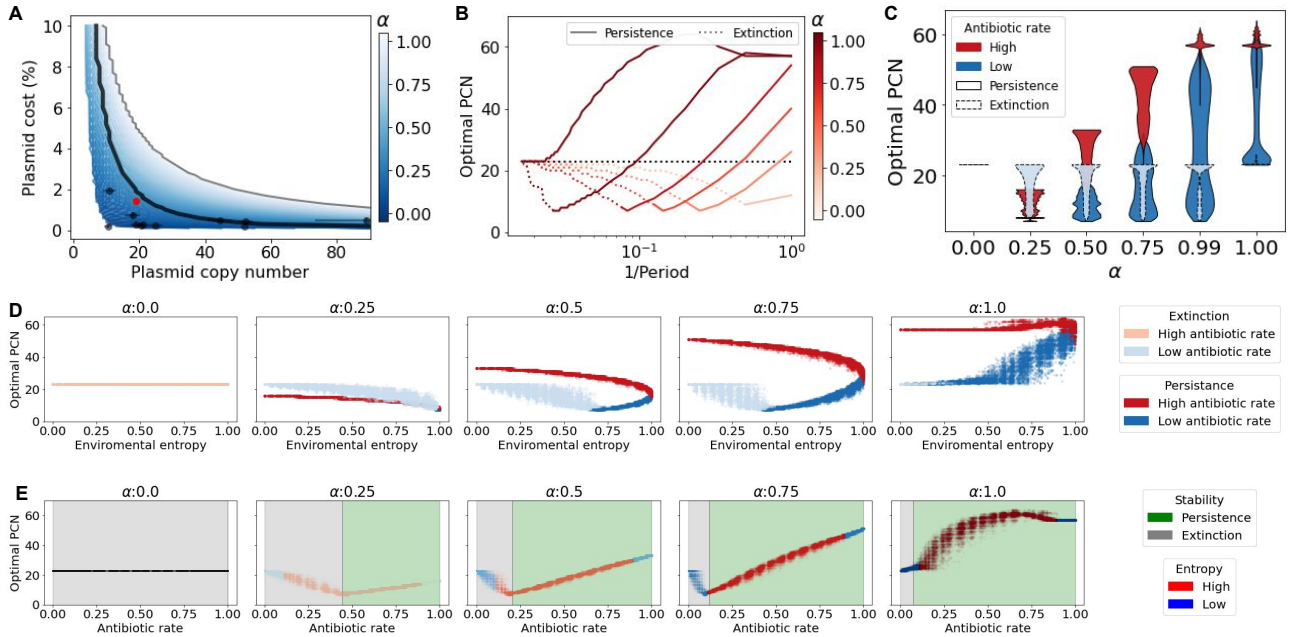

Figure 5. Optimal PCNs in fluctuating environments. A) Optimal PCN as the number of copies that maximizes the area under the curve of Figure 1B, the optimal PCN decreases exponentially as we increase the fitness cost associated with carrying plasmids, as indicated in black-solid line. Black dots show some PCN-costs data obtained from the literature. Red dots indicate the values of pBGT. Blue-scale lines indicate optimal PCN curves for many values of α. Light-blues indicate higher values of α whereas dark-blues indicate lower values of α. Gray line shows the max PCN for the corresponding plasmid cost. **B)** Optimal PCN in periodic environments. Each curve corresponds to a value of α. Black line shows $\alpha = 0$. Observe that for very short periods optimal PCNs are high, then for certain period the optimal PCN reaches a minimum then as period increases, the optimal PCN tends to the optimal of $\alpha = 0$. **C-E)** Optimal PCNs using random environments. **C)** Environments are classified by their rate of days with antibiotics, the rate differences produce a multi-modal outcome, where higher rates increases the optimal PCN and vice-versa. Simulations using the same environments were made for different αs. Note that α intensity increases the separation of the modes. Modes are also classified by their stability, persistence marked with a solid border line and extinction with a dashed border line. **D)** Panel of optimal PCNs plotted by the environment entropy for sample α. Environments are classified by their antibiotic rate. **E)** Panel of optimal PCNs plotted by the environment antibiotic rate for sample α. Environments are classified by their entropy.

3 Discussion

In this work, we have used a population genetics model to study how non-transmissible plasmids are maintained in a bacterial population. In particular, we consider small multi-copy plasmids that lack active partitioning mechanisms. The model has the following biological implications: 1) Plasmids encode for accessory genes that confer an advantage in harsh environments, for instance antibiotic resistance genes; 2) Bearing plasmids represents a fitness cost associated to plasmid replication and maintenance; 3) Each plasmid is segregated randomly to a daughter cell upon division; thus, plasmid bearing bacteria can produce plasmid-free cells with a probability of $1/2^n$, were n is the plasmid copy number.

We validated our model using a well characterized model plasmid, pBGT.[21,34,35] By analyzing growth kinetics of the plasmid-bearing and the plasmid-free strains we estimated the maximal growth rates of both strains, as well as the fitness cost associated to plasmid bearing and the fitness advantage of the plasmid bearing cells for different antibiotic concentrations. By numerically solving our model with parameters obtained from the experimental data, we found that selection is necessary for persistence of costly plasmids. In other words, both our model and data suggest that plasmid-bearing strains found in nature have necessarily been exposed to antibiotics (or other forms of positive selection) in the past.

By studying the dynamics under different antibiotics concentrations, we found that the strength of selection is highly correlated with the final fraction of plasmids in the entire population. Consequently, we also found that there is a trade-off between selection strength and plasmid cost, i.e. the cost per plasmid and the plasmid copy number. Whether plasmids are maintained or lost in the long term results from the complex interplay between plasmid copy number and its fitness cost, as well as the intensity, and frequency of positive selection. These relationships are not necessarily linear, as seen in the exhaustive exploration a wide-range of parameters combinations performed in this study. We argue that this model could be easily applied to make informed decisions for a specific plasmid maintenance, for instance for biotechnological purposes or to design rational sequential treatments that control plasmid-borne antibiotic resistance in clinical settings.

When we considered random environments, we observed that the optimal PCN depends on the strength of selection, the frequency at which antibiotics are administered (antibiotic rate) and environmental entropy, in a non-linear manner. In particular, we observed that fixed values of the strength of selection yield to a multi-modal distribution of the optimal PCN, depending the antibiotic rate in the environment (Figure 5C). Multi-modality of plasmid size distribution had previously been described in[39] for non-transmissible plasmids and in[40] for conjugative plasmids. We obtained data from the literature[34,41–43] and explored the correlation between plasmid copy number and plasmid size. As expected, we obtained a negative correlation between plasmid size and copy number (Pearson correlation coefficient $= -0.876$, p-value= $8.3\text{x}10^{-06}$; see Appendix B). In this direction, classic methods for

plasmid copy number estimation correlate plasmid size with PCN.[44] Additionally, it has been observed that inserting foreign DNA of different sizes into the same plasmid, the size of the insertions correlates with a decrease in copy number.[42,45] This is in line with the correlation between optimal PCN and plasmid cost that we observe in our model.

In summary, we have showed that a trade-off between segregational loss and plasmids cost implies the existence of an optimal plasmid copy number, which depends on the plasmid cost, as well as the strength and mode of selection (constant, periodic or random). Therefore, at least in principle, if a plasmid-bearing bacterial population is found in natural conditions, under the assumption that the number of plasmids is close to optimal, the environmental conditions that the colony has experienced can be estimated using our model. Finally, our conclusion should hold for non-random segregation (e.g. active partitioning), as this would decrease the probability of segregational loss (which corresponds to having a smaller value of μ_n in our model) so, as reported in,[46] its optimal copy number will likely be lower than a plasmid that relies on random segregation.

4 Data availability

The data and code underlying this article are available at https://doi.org/10.5281/zenodo.6360056

5 Acknowledgements

We thank A San Millan for the generous gift of the strains and for useful discussions. VMP acknowledges support of the Spanish Ministry of Science and Innovation to the EMBL partnership, the Centro de Excelencia Severo Ochoa and the CERCA Programme / Generalitat de Catalunya. VMP was also funded by the DGAPA-UNAM postdoctoral program. JCRHB was a doctoral student in Programa de Doctorado en Ciencias Biomédicas, Universidad Nacional Autónoma de México, and received fellowship 59691 from CONACYT. ASJ was supported by PAPIIT-UNAM (grant IA103820). RPM was supported by PAPIIT-UNAM (grant IN209419) and by CONACYT Ciencia Básica (grant A1-S-32164). AGC was supported by PAPIIT-UNAM (grant IN101722) and by CONACYT Ciencia Básica (grant A1-S-14615). The corresponding author was elected between the four PIs by means of a horse race where the winner horse was named Guilty Pleasure.

References

1. Chen, J. *et al.* Genome hypermobility by lateral transduction. *Science* **362**, 207–212 (2018).
2. Chen, I. & Dubnau, D. Dna uptake during bacterial transformation. *Nature Reviews Microbiology* **2**, 241–249 (2004).

3. Funnell, B. E. & Phillips, G. *Plasmid biology*, vol. 672 (ASM press Washington, DC, 2004).

4. Groisman, E. A. & Ochman, H. Pathogenicity islands: bacterial evolution in quantum leaps. *Cell* **87**, 791–794 (1996).

5. Alonso, J. C. & Tolmasky, M. E. *Plasmids: biology and impact in biotechnology and discovery* (John Wiley & Sons, 2020).

6. Pemberton, J. & Don, R. Bacterial plasmids of agricultural and environmental importance. *Agriculture and Environment* **6**, 23–32 (1981).

7. San Millan, A. Evolution of plasmid-mediated antibiotic resistance in the clinical context. *Trends in microbiology* **26**, 978–985 (2018).

8. Baltrus, D. A. Exploring the costs of horizontal gene transfer. *Trends in ecology & evolution* **28**, 489–495 (2013).

9. San Millan, A. & Maclean, R. C. Fitness costs of plasmids: a limit to plasmid transmission. *Microbiology spectrum* **5** (2017).

10. Vogwill, T. & MacLean, R. C. The genetic basis of the fitness costs of antimicrobial resistance: a meta-analysis approach. *Evolutionary applications* **8**, 284–295 (2015).

11. Stewart, F. M. & Levin, B. R. The population biology of bacterial plasmids: a priori conditions for the existence of conjugationally transmitted factors. *Genetics* **87**, 209–228 (1977).

12. Bergstrom, C. T., Lipsitch, M. & Levin, B. R. Natural selection, infectious transfer and the existence conditions for bacterial plasmids. *Genetics* **155**, 1505–1519 (2000).

13. Mochizuki, A., Yahara, K., Kobayashi, I. & Iwasa, Y. Genetic addiction: selfish gene's strategy for symbiosis in the genome. *Genetics* **172**, 1309–1323 (2006).

14. Salje, J. Plasmid segregation: how to survive as an extra piece of dna. *Critical reviews in biochemistry and molecular biology* **45**, 296–317 (2010).

15. Hall, J. P., Wood, A. J., Harrison, E. & Brockhurst, M. A. Source–sink plasmid transfer dynamics maintain gene mobility in soil bacterial communities. *Proceedings of the National Academy of Sciences* **113**, 8260–8265 (2016).

16. Paulsson, J. & Ehrenberg, M. Trade-off between segregational stability and metabolic burden: a mathematical model of plasmid cole1 replication control. *Journal of molecular biology* **279**, 73–88 (1998).

17. Paulsson, J. Multileveled selection on plasmid replication. *Genetics* **161**, 1373–1384 (2002).

18. Garoña, A., Hülter, N. F., Romero Picazo, D. & Dagan, T. Segregational drift constrains the evolutionary rate of prokaryotic plasmids. *Molecular Biology and Evolution* (2021).

19. Rodríguez-Beltrán, J., DelaFuente, J., León-Sampedro, R., MacLean, R. C. & San Millán, Á. Beyond horizontal gene transfer: the role of plasmids in bacterial evolution. *Nature Reviews Microbiology* 1–13 (2021).

20. Santer, M. & Uecker, H. Evolutionary rescue and drug resistance on multicopy plasmids. *Genetics* **215**, 847–868 (2020).

21. Rodriguez-Beltran, J. *et al.* Multicopy plasmids allow bacteria to escape from fitness trade-offs during evolutionary innovation. *Nature ecology & evolution* **2**, 873 (2018).

22. Ilhan, J. *et al.* Segregational drift and the interplay between plasmid copy number and evolvability. *Molecular biology and evolution* **36**, 472–486 (2019).

23. Rodriguez-Beltran, J. *et al.* Genetic dominance governs the evolution and spread of mobile genetic elements in bacteria. *bioRxiv* 863472 (2019).

24. Salverda, M. L., De Visser, J. A. G. & Barlow, M. Natural evolution of tem-1 β-lactamase: experimental reconstruction and clinical relevance. *FEMS microbiology reviews* **34**, 1015–1036 (2010).

25. Baake, E., Cordero, F. & Hummel, S. A probabilistic view on the deterministic mutation–selection equation: dynamics, equilibria, and ancestry via individual lines of descent. *Journal of mathematical biology* **77**, 795–820 (2018).

26. Chevin, L.-M. On measuring selection in experimental evolution. *Biology letters* **7**, 210–213 (2011).

27. González Casanova, A., Kurt, N., Wakolbinger, A. & Yuan, L. An individual-based model for the Lenski experiment, and the deceleration of the relative fitness. *Stochastic Processes and their Applications* **126**, 2211–2252 (2016).

28. Gerrish, P. & Lenski, R. The fate of competing beneficial mutations in an asexual population. *Genetica* **102** (1998).

29. Baake, E., Casanova, A. G., Probst, S. & Wakolbinger, A. Modelling and simulating Lenski's long-term evolution experiment. *Theoretical population biology* **127**, 58–74 (2019).

30. Kumar, P., Maschke, H., Friehs, K. & Schügerl, K. Strategies for improving plasmid stability in genetically modified bacteria in bioreactors. *Trends in biotechnology* **9**, 279–284 (1991).

31. Yurtsev, E. A., Chao, H. X., Datta, M. S., Artemova, T. & Gore, J. Bacterial cheating drives the population dynamics of cooperative antibiotic resistance plasmids. *Molecular systems biology* **9**, 683 (2013).

32. Harrison, E., Guymer, D., Spiers, A. J., Paterson, S. & Brockhurst, M. A. Parallel compensatory evolution stabilizes plasmids across the parasitism-mutualism continuum. *Current Biology* **25**, 2034–2039 (2015).

33. San Millan, A., Heilbron, K. & MacLean, R. C. Positive epistasis between co-infecting plasmids promotes plasmid survival in bacterial populations. *The ISME journal* **8**, 601–612 (2014).

34. San Millan, A., Escudero, J. A., Gifford, D. R., Mazel, D. & MacLean, R. C. Multicopy plasmids potentiate the evolution of antibiotic resistance in bacteria. *Nature ecology & evolution* **1**, 1–8 (2016).

35. Hernandez-Beltran, J., Rodríguez-Beltrán, J., San Millán, A., Peña-Miller, R. & Fuentes-Hernández, A. Quantifying plasmid dynamics using single-cell microfluidics and image bioinformatics. *Plasmid* 102517 (2020).

36. Hall, B. G., Acar, H., Nandipati, A. & Barlow, M. Growth rates made easy. *Molecular biology and evolution* **31**, 232–238 (2014).

37. Stevenson, C., Hall, J. P., Brockhurst, M. A. & Harrison, E. Plasmid stability is enhanced by higher-frequency pulses of positive selection. *Proceedings of the Royal Society B: Biological Sciences* **285**, 20172497 (2018).

38. Herencias, C. *et al.* Collateral sensitivity associated with antibiotic resistance plasmids. *Elife* **10**, e65130 (2021).

39. Smillie, C., Garcillán-Barcia, M. P., Francia, M. V., Rocha, E. P. & de la Cruz, F. Mobility of plasmids. *Microbiol. Mol. Biol. Rev.* **74**, 434–452 (2010).

40. Ledda, A. & Ferretti, L. A simple model for the distribution of plasmid lengths. *arXiv preprint arXiv:1411.0297* (2014).

41. Zhong, C. *et al.* Determination of plasmid copy number reveals the total plasmid dna amount is greater than the chromosomal dna amount in bacillus thuringiensis ybt-1520. *PloS one* **6**, e16025 (2011).

42. Smith, M. A. & Bidochka, M. J. Bacterial fitness and plasmid loss: the importance of culture conditions and plasmid size. *Canadian journal of microbiology* **44**, 351–355 (1998).

43. San Millan, A. *et al.* Positive selection and compensatory adaptation interact to stabilize non-transmissible plasmids. *Nature communications* **5**, 5208 (2014).

44. Friehs, K. Plasmid copy number and plasmid stability. *New trends and developments in biochemical engineering* 47–82 (2004).

45. Warnes, A. & Stephenson, J. R. The insertion of large pieces of foreign genetic material reduces the stability of bacterial plasmids. *Plasmid* **16**, 116–123 (1986).

46. Lopez, J., Donia, M. & Wingreen, N. Modeling the ecology of parasitic plasmids. *ISME J.* **15**, 2843–2852 (2021).

47. Etheridge, A. *Some Mathematical Models from Population Genetics: École D'Été de Probabilités de Saint-Flour XXXIX-2009*, vol. 2012 (Springer Science & Business Media, 2011).

48. Athreya, K. B. & Ney, P. E. *Branching processes*, vol. 1 (Dover Publications, Inc., Mineola, NY, 2004).

49. R Core Team. *R: A Language and Environment for Statistical Computing*. R Foundation for Statistical Computing, Vienna, Austria (2020). URL https://www.R-project.org.

50. Petzoldt, T. *Estimate Growth Rates from Experimental Data* (2019). URL https://CRAN.R-project.org/package=growthrates. R package version 0.8.1.

51. Santos-Lopez, A. *et al.* Compensatory evolution facilitates the acquisition of multiple plasmids in bacteria. *bioRxiv* 187070 (2017).

52. Harrison, E., Koufopanou, V., Burt, A. & Maclean, R. The cost of copy number in a selfish genetic element: the 2-μm plasmid of s accharomyces cerevisiae. *Journal of evolutionary biology* **25**, 2348–2356 (2012).

6 Appendix A: Mathematical model

6.1 Fixed points of equation (2)

Let $\overline{f} = f \circ g$. We want to study the fixed points of $\overline{f}$ and their domains of attraction. It is not hard to see that 0 is always a stable fixed point. In addition, if $x \neq 0$,

$$\begin{aligned}
& \overline{f}(x) = \frac{x(1-\kappa_n)(1-\mu_n)/(\alpha-\kappa_n)}{(1-\alpha)/(\alpha-\kappa_n)+x} = x \\
\Leftrightarrow \quad & x^2 + \frac{1-\alpha}{\alpha-\kappa_n}x = \frac{(1-\kappa_n)(1-\mu_n)}{\alpha-\kappa_n}x \\
\Leftrightarrow \quad & x = \frac{(1-\kappa_n)(1-\mu_n)-(1-\alpha)}{\alpha-\kappa_n} = 1-\mu_n\frac{1-\kappa_n}{\alpha-\kappa_n}.
\end{aligned}$$

Denote $x^* := 1-\mu_n(1-\kappa_n)/(\alpha-\kappa_n)$. Since the frequencies are in $[0,1]$, this fixed point only exists if $\alpha > \kappa_n + \mu_n(1-\kappa_n)$. As n increases, μ_n decreases exponentially, while κ_n increases only linearly, so there is a non linear relationship between n and the minimun α required for the existence of a second fixed point x^*.

Let us analyze the stability of x^*. Let us assume that $\alpha > \kappa_n + \mu_n(1-\kappa_n)$.

$$\begin{aligned}
& \overline{f}(x) - x = \frac{x(1-\kappa_n)(1-\mu_n)/(\alpha-\kappa_n) - x(1-\alpha)/(\alpha-\kappa_n) - x^2}{(1-\alpha)/(\alpha-\kappa_n)+x} > 0 \\
\Leftrightarrow \quad & \frac{(1-\kappa_n)(1-\mu_n)}{(\alpha-\kappa_n)} - \frac{1-\alpha}{\alpha-\kappa_n} - x > 0 \\
\Leftrightarrow \quad & x < x^*.
\end{aligned}$$

So, the frequency increases if it is below x^* and decreases otherwise, meaning that it is a stable fixed point. In addition, the domain of attraction is $(0,1]$, meaning that this equilibrium fraction is reached for any initial state.

To sum up, if $\alpha < \kappa_n + \mu_n(1-\kappa_n)$ there is only one fixed point, 0, which is stable. If $\alpha > \kappa_n + \mu_n(1-\kappa_n)$ then there are two stable fixed points, 0 and x^*.

6.2 Choice of the model

In this section, we compare two types of mathematical models for the evolution of plasmid-bearing frequencies, the discrete time model used in this paper and the Wright-Fisher diffusion.

Let us assume that the mutation rate $\mu_{N,n} = 2^{-n}$ and the cost $\kappa_{N,n}$ are parametrized by N. To see the accumulated effects of plasmid cost, segregational loss and genetic drift, we need $\kappa_{N,n}$ and $\mu_{N,n}$ to

be of order $1/N$ (see e.g. Chapter 5 in[47]). The first condition is fulfilled if the cost per plasmid is very low, for example when $\kappa_{N,n} = \kappa n/N$. The second one stands if n is of order $\log_2(N)$, which is the case, for example, if $n = 20$ and $N = 10^6$, or if $n = 15$ and $N = 10^5$. In that case we set $\mu = N2^{-n}$. Under this setting, when time is accelerated by N, the frequency process of individuals with plasmids can be approximated by the solution of the stochastic differential equation (SDE)

$$dX_t = -\mu X_t dt - \kappa X_t(1-X_t)dt + \sqrt{X_t(1-X_t)}dB_t, \tag{4}$$

where B is a standard Brownian motion. This is known as the Wright-Fisher diffusion with mutation and selection. When antibiotic is added, at times $\{T, 2T, \dots\}$, then (4) modifies to

$$dX_t = \sum_{j\geq 1} \frac{\alpha X_{jT-}(1-X_{jT-})}{1-\alpha(1-X_{jT-})}\mathbf{1}_{jT\leq t} - \mu X_t dt - \kappa X_t(1-X_t)dt + \sqrt{X_t(1-X_t)}dB_t. \tag{5}$$

However, in our experimental setting, the cost that we measure ($\kappa_n \simeq 0.27$) is much higher than the inverse population size, so we are in the regime of strong selection. In other words, for plasmids that have a very small cost, of the order of $1/N$, genetic drift would play an important role, and the above Wright-Fisher diffusion with mutation, selection and antibiotic peaks (5) would be the most suitable model. But in our setting, selection (plasmid cost) is so high that genetic drift becomes negligible. Recall that equation (2) does not need any time rescaling, whereas, in the diffusion (5) time is measured in units of N generations. Under strong selection, the frequencies evolve much faster.

From the Wright-Fisher model to the serial dilution protocol

In this section we provide some details on how to parametrize our model (equation (2)) to adapt to our experimental setting.

Intraday dynamics. Day i starts with N founder individuals ($N \sim 10^5$ in the experiment) and reproduction stops when saturation is reached, which corresponds to a population size of γN ($\gamma N \sim 10^7$ in the experiment). Among the founder individuals, there is a fraction x of plasmid-free cells. We assume that, in the absence of antibiotic, the population evolves as a continuous time multi-type branching process $\mathbf{Z}_t = (Z_t^0, Z_t^1)$ where the reproduction rate (or *Malthusian fitness*) of PB (resp. PF) individuals is r (resp. $r+\rho$), with $\rho > 0$ (since PB individuals have some disadvantage due to the cost of plasmid maintenance).

Following,[27] we assume that $\rho \sim N^{-b}$ for some $b \in (0, 1/2)$ (this regime is known as *moderate-strong selection*). In every branching event, an individual splits in two. Plasmid-free individuals only split in two PF individuals. Plasmid-bearing individuals can split in one PF individual and one PB individual with probability 2^{-n} (if all the plasmids go to one of them) or they can split in two plasmid-bearing individuals with probability $1-2^{-n}$. Let $M(t) = \{M_{i,j}(t) : i, j = 0, 1\}$ be the mean

matrix given by $M_{i,j}(t) = \mathbb{E}_{\mathbf{e}_i}(Z_t^j)$, the average size of the type j population at time t if we start with a type i individual. According to [48, Section V.7.2], $M(t)$ can be calculated as an exponential matrix

$$M(t) = e^{tA} \qquad \text{where} \qquad A = \begin{pmatrix} r+\rho & 0 \\ r2^{-n} & r(1-2^{-n}) \end{pmatrix}.$$

More precisely,

$$M(t) = \begin{pmatrix} e^{(r+\rho)t} & 0 \\ \frac{r2^{-n}}{r2^{-n}+\rho}(e^{(r+\rho)t} - e^{r(1-2^{-n})t}) & e^{r(1-2^{-n})t} \end{pmatrix}.$$

Let σ be the duration of the growth phase. Since N is very large, one can assume that reproduction is stopped when the expectation of the number of descendants reaches γN, i.e. that σ satisfies

$$\begin{aligned} \gamma N =& (1-x)N(M_{0,0}(\sigma) + M_{0,1}(\sigma)) + xN(M_{1,0}(\sigma) + M_{1,1}(\sigma)) \\ =& Ne^{r\sigma}\left(e^{\rho\sigma} + \rho x\,\frac{e^{-r2^{-n}\sigma} - e^{\rho\sigma}}{r2^{-n}+\rho}\right). \end{aligned}$$

Since $\rho \sim N^{-b}$, we have for large enough N that

$$\sigma \simeq \frac{\log\gamma}{r}.$$

Interday dynamics. We consider a discrete time model, with fixed population size N, in which generation i corresponds to the founder individuals of day i. Suppose that the frequency of plasmid-bearing individuals in generation i is x. To form generation $i+1$ we sample N individuals from the γN individuals present at the end of day i . Since γ is large enough, we can assume that individuals are sampled with replacement. The probability that an individual in the sample is PB is equal to

$$\frac{xM_{1,1}(\sigma)}{(1-x)(M_{0,0}(\sigma)+M_{0,1}(\sigma)) + x(M_{1,0}(\sigma)+M_{1,1}(\sigma))} = \frac{xe^{-(r2^{-n}+\rho)\sigma}}{(1-x) + x\frac{r2^{-n}+\rho e^{-(r2^{-n}+\rho)\sigma}}{r2^{-n}+\rho}}. \tag{6}$$

This is equal to the probability of choosing a PB parent in the Wright-Fisher model introduced above, with

$$\kappa_n = \frac{\rho(1-e^{-(r2^{-n}+\rho)\sigma})}{r2^{-n}+\rho} \qquad \text{and} \qquad \mu_n = 1 - \frac{r2^{-n}+\rho}{r2^{-n}e^{(r2^{-n}+\rho)\sigma}+\rho}. \tag{7}$$

7 Appendix B: Methods

Bacterial strains and media

The plasmid free strain we used was *E. coli* K12 MG1655 and the plasmid bearing strain was MG/pBGT[34] carrying the multi-copy plasmid pBGT with the β-lactamase $bla_{\text{TEM-1}}$ which confers resistance to ampicillin and the fluorescent protein GFP under an arabinose inducible promoter.

Overnight cultures were grown in flasks with 20 ml of lysogeny broth (LB) (Sigma L3022) with 0.5 % w/v L-(+)-Arabinose (Sigma A91906) for fluorescence induction, in a shaker-incubator at 220 RPM at 37 C. For the plasmid bearing strain, 25 mg/l of ampicillin (Sigma A0166) were added to eliminate segregants. Ampicillin stock solutions were prepared at 100 mg/ml directly in LB and sterilized by 0.22 μm (Millex-GS SLGS033SB) filtering. Arabinose stock solutions were prepared at 20% w/v in DD water and sterilized by filtration.

To construct our inoculation plate, overnight cultures of the plasmid-free strain and the plasmid bearing strain were adjusted to 1 OD (630 nm) using a BioTek ELx808 Absorbance Microplate Reader diluted with fresh ice cooled LB. Appropriate volumes were mixed to make co-cultures at fractions 0, 0.1, 0.2, ..., 1 and set column-wise on a 96-well plate (Corning CLS3370).

Competition experiments were performed using 96-well plates with 200 μl of LB with 0.5% w/v arabinose, and respective ampicillin concentrations: 0, 1, 2, 2.5, 3, 3.5, 4, and 6 mg/l was implemented by plate rows. Antibiotic plates were inoculated using a 96 Pin microplate replicator (Boekel 140500), flame sterilization was made before each inoculation. Four replicates plates were grown in static incubator at 37$^{\circ}C$. After 24 hours growth, plates were read in a fluorescence microplate reader (BioTek Synergy H1) using OD (630 nm) and eGFP (479,520 nm) after 1 minute shaking.

Growth kinetics measurements were performed in 96 well plates with 200 μl of LB with 0.5% w/v arabinose without antibiotics, plates were sealed using X-Pierce film (Sigma Z722529), each well seal film was pierced in the middle with a sterile needle to avoid condensation. Plates were grown at 37 deg$C$ and reading for OD and fluorescence were made every 20 minutes after 30 seconds linear shaking.

Plasmid fraction determination

To calculate fluorescence intensity values, we first subtracted the background signal of LB for fluorescence and OD respectively, then the debackgrounded fluorescence signal was scaled dividing by the debackgrounded OD. The measurements for our inoculation plate showed a strong linear correlation ($R^2 = 0.995$) between co-cultures fractions and fluorescence intensity (Figure 3A). This allowed to directly approximate the populations plasmid fractions from the readings of our competition experiments. We normalized the data independently for each antibiotic concentration taking

the average measurements of the 4 replicates. Plasmid fractions, PF, were inferred by normalizing the mean fluorescence intensity for each well, f_i, to the interval [0,1] using the following formula: $PF_i = (f_i - f_{min})/(f_{max} - f_{min})$ were f_{max} and f_{min} are the mean fluorescence intensities at fractions 1 and 0 respectively.

Parameter estimation

Model kinetics parameters were estimated using the R[49] package growth rates.[50] Exponential phase duration, σ, was calculated by finding lag phase duration using the linear model and the time to reach carrying capacity, found using the non-linear growth model Baranyi. Maximum growth rates, r and $r+\rho$, were estimated using the smooth spline method. κ_n value was estimated using equation (1) and the data from the antibiotic-free competition experiment using a curve fitting algorithm from the SciPy library in a custom Python script. Respective values of α were found in the same manner using equation (2) and fixing κ_n. κ_n was also calculated using the formula in equation 3 with a very similar result. The parameters are summarized in Tables 1 and 2.

Random environments

Environmental sequences of size 1000 (days) using a binomial distribution varying the probability of success. For each environment created we also bit-flipped (so 101... turns into 010...) and two measures was applied to each resulting environments. First, we used Shannon entropy, $H(Env) = -\sum_i^n p_i log_n(p_i)$, with two states, $n = 2$ (antibiotic or no-antibiotic) and p_i equal to the probability of finding an state day, i.e. the fractions of days with antibiotics and without antibiotics. We classified environments by their H and by the fraction of antibiotic days, as being this an important feature. This two measures are in the [0,1] interval so we binned the intervals into 20 bins and 1,000 environments were created for each bin.

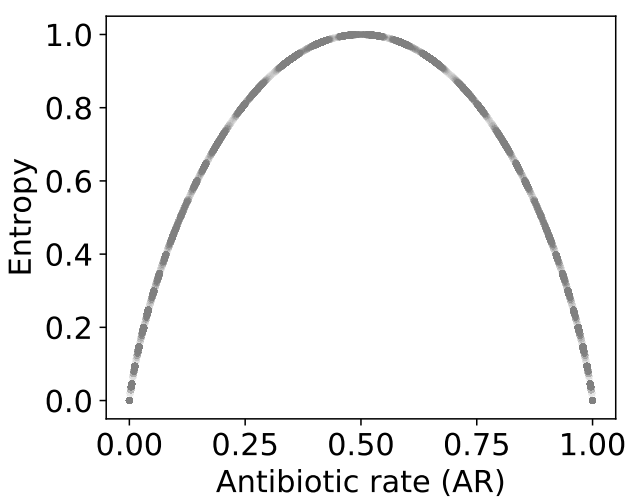

Sup. Figure 1. Relationship between random environments antibiotic rate and Entropry.

Simulations details

The model was implemented in Python, using standard scientific computing libraries (Numpy, MatplotLib, and the Decimal library was required to resolve small numbers conflicts). In general, all simulations started at PB frequency 1, with the exceptions of figure 2 and 4D. Numeric simulations were defined to reach a steady state the first time a value is repeated. In the case of periodic environments, the repetition must happen at antibiotics peaks days. We considered extinction if the end point of the realization dropped below a threshold adjusted to the simulations times, the highest being $1x10^{-7}$ and the lowest $1x10^{-100}$.

Plasmid size and copy number association

We searched the literature for articles where both plasmid copy number and plasmid size had been measured. We found a strong negative correlation between the logarithms of these two quantities (Pearson correlation coefficient of -0.876, Sup. Figure 2). Data is summarized in Table 4.

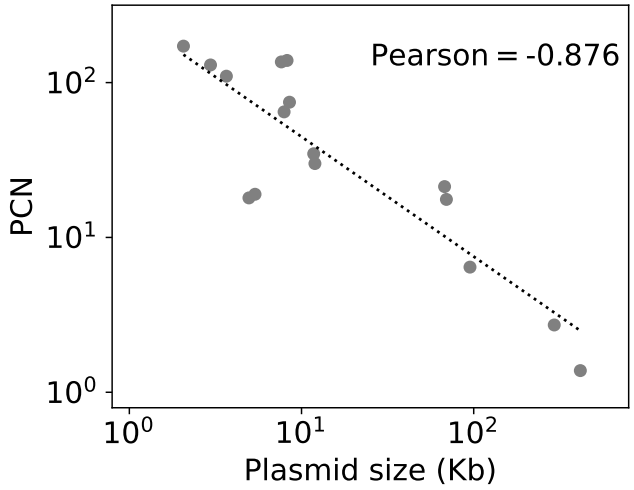

Sup. Figure 2. Plasmid size and plasmid copy number (log-log scale). Data from references in Table 4.

Tables

Parameter	Measured value	Formula	Estimated value	Description
r	0.435435	NA	NA	plasmid strain growth rate
ρ	0.052334	NA	NA	WT growth rate advantage
σ	6.074089	NA	NA	exponential phase duration
μ_n	NA	$\mu_n = 1 - \frac{r2^{-n}+\rho}{r2^{-n}e^{(r2^{-n}+\rho)\sigma}+\rho}$	5.938e-06	1-day fraction of segregants
κ_n	NA	$\kappa_n = \frac{\rho(1-e^{-(r2^{-n}+\rho)\sigma})}{r2^{-n}+\rho}$	0.272313	fitness cost
n	19	NA	NA	plasmid copy number

Table 1. Model kinetic parameters

Amp	κ_n	α
0.0	0.272276	0.0
1.0	0.272276	-0.37781
2.0	0.272276	-0.332662
2.5	0.272276	-0.058457
3.0	0.272276	0.992911
3.5	0.272276	0.9801
4.0	0.272276	0.992075
6.0	0.272276	0.99373

Table 2. Selection parameters

Name	Plasmid Type	Species	PCN	PCN SD	Cost	Cost SD	Reference
pB1006	ColE1	*Haemophilus influenzae* RdKW20	10.530	1.112	0.021	0.012	[51]
pB1005	ColE1	*Haemophilus influenzae* RdKW20	20.450	2.590	0.05	0.013	[51]
pB1000	ColE1	*Haemophilus influenzae* RdKW20	25.020	1.920	0.054	0.002	[51]
pNI105		*Pseudomonas aeruginosa*	18.000	2.400	0.132	0.025	[33]
2-uM		*Saccharomyces cerevisiae*	52.000	0.000	0.0884	0.00416	[52]
pNUK73		*Pseudomonas aeruginosa*	11.030	1.890	0.214	0.008	[33]
pBGT	ColE1	*Escherichia coli*	19.120	1.560	0.057	0.013	[34]
pBGT R164S	ColE1	*Escherichia coli*	21.100	0.850	0.057	0.003	[34]
pBGT G54U	ColE1	*Escherichia coli*	44.500	3.810	0.207	0.019	[34]
pBGT G55U	ColE1	*Escherichia coli*	88.930	15.650	0.443	0.116	[34]
pBGT R164S G54U	ColE1	*Escherichia coli*	52.300	2.190	0.238	0.016	[34]
pBGT R164S G55U	ColE1	*Escherichia coli*	127.290	4.580	0.491	0.082	[34]

Table 3. Plasmid copy number and plasmid costs from literature. SD Standard Deviation.

Name	Plasmid Type	Species	PCN Mean	PCN SD	Size (Kb)	Reference
pBMB2062	RCR	*B. thuringiensis*	172	5.67	2.062	[41]
pBMB7635	RCR	*B. thuringiensis*	136	6.36	7.635	[41]
pBMB7921	RCR	*B. thuringiensis*	64.7	1.12	7.921	[41]
pBMB8240	?	*B. thuringiensis*	139	1.76	8.24	[41]
pBMB8513	RCR	*B. thuringiensis*	74.7	1.44	8.513	[41]
pBMB11	RCR	*B. thuringiensis*	34.7	0.69	11.769	[41]
pBMB67	θ	*B. thuringiensis*	21.3	1.06	67.73	[41]
pBMB69	θ	*B. thuringiensis*	17.6	0.7	69.416	[41]
pBMB95	θ	*B. thuringiensis*	6.43	0.09	95.15	[41]
pBMB293	?	*B. thuringiensis*	2.72	0.16	293.574	[41]
pBMB400	?	*B. thuringiensis*	1.38	0.14	416.21	[41]
pBluescript	ColE1 (derivative) and F1	*E. coli* XL1Blue	130	0	2.961	[42]
pBluescript+700	ColE1 (derivative) and F2	*E. coli* XL1Blue	110	0	3.661	[42]
pBluescript+9000	ColE1 (derivative) and F3	*E. coli* XL1Blue	30	0	11.961	[42]
pNI105	pSC101?	*P. aeruginosa* PAO1	18	2.4	4.95	[33]
pBGT	ColE1	*E. coli*	19	1.56	5.369	[34]

Table 4. Plasmid copy number and plasmid size from literature. SD Standard Deviation. RCR Rolling Circle Replication.